Theoretical Studies of Organometallic Compounds. 5. Alkyne and Vinylidene Complexes of Molybdenum and Tungsten in High-Oxidation States[1]

Ralf Stegmann, Arndt Neuhaus, and Gernot Frenking*

Contribution from the Fachbereich Chemie, Universität Marburg, Hans-Meerwein-Strasse, D-35032 Marburg, Germany

Received March 11, 1993®

Abstract: The geometries of the acetylene complexes $MX_4C_2H_2$ and the vinylidene isomers MX_4CCH_2 (M = W, Mo; X = F, Cl) are theoretically predicted using quantum mechanical ab initio methods at the Hartree–Fock level of theory and relativistic effective core potentials for the transition metals. The optimized geometries and energies of the anionic complexes $MX_5C_2H_2^-$ are also reported. The optimization of $WX_5C_2H_2^-$ gives geometries for the chloro and fluoro complexes, which are in good agreement with experiment. The corresponding $MoX_5C_2H_2^-$ structures are not minima on the potential energy surface. The geometries and energies of the alkyne complexes are compared with the optimized structures of the vinylidene complexes. The vinylidene complexes are calculated to be slightly higher in energy than the alkyne complexes, but they become clearly more stable than the alkyne complexes when hydrogen is substituted by fluorine. The electronic structure of the complexes is investigated using the natural bond orbital population analysis and the topological analysis of the wave function. Detailed information is given about the nature of the metal–carbon bonds and the hybridization and atomic population of the transition metals in the alkene and vinylidene complexes.

Introduction

Transition-metal chlorides such as WCl_6 and $MoCl_5$ are effective catalysts for the polymerization of acetylene.[2–6] The properties of the polymer[7–10] such as tacticity and conductivity are strongly influenced by the chosen catalyst system. Although the transition-metal-catalyzed acetylene polymerization is a chemically and industrially important reaction, little is known about the catalytic mechanism. It has been suggested that alkyne complexes of transition metals with a side-on coordinated ligand may be formed as intermediates in the cyclooligomerization[11–14] and polymerization[15] of alkynes and related reactions.

In the last few years, the isolation and characterization of alkyne complexes of tungsten, rhenium, osmium, and molybdenum in high-oxidation states were achieved by reaction of the transition-metal chlorides with the alkyne in the presence of a reductive reactant which could be the alkyne itself.[16–22]

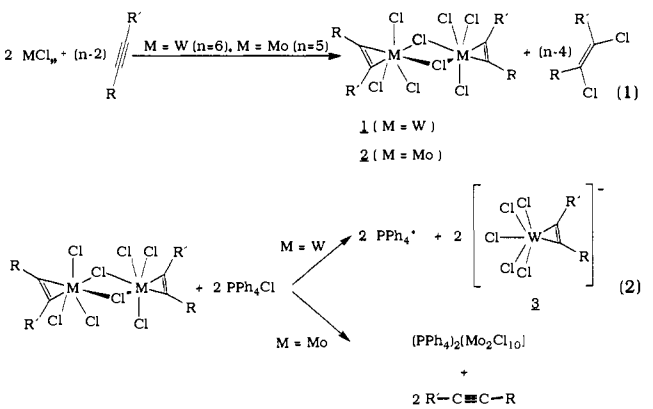

(1)

(2)

Figure 1. Reaction schemes for reactions 1 and 2.

Many transition-metal–alkyne complexes could be characterized by infrared and NMR spectroscopy. The geometries of several complexes were determined by X-ray structure analyses.[16–22] Although these complexes have very similar geometries, they exhibit different chemical behaviors with various reagents. In particular, the stability against solvents and further addition of chloride ions varies considerably.[17] For example, the dimeric tungsten–alkyne complex **1** reacts with tetraphenylphosphonium chloride to give the stable monomeric complex **3** (Figure 1). The analogous molybdenum complex **2** loses the alkyne ligands to form an anionic dimeric chloro complex (Figure 1). Also, some

® Abstract published in *Advance ACS Abstracts*, September 15, 1993.

(1) For Part 4, see: Jonas, V.; Frenking, G.; Reetz, M. T. *Organometallics*, in press.

(2) Aldissi, M.; Linaya, C.; Sledz, J.; Schue, F.; Giral, L.; Fabre, J. M.; Rolland, M. *Polymer* **1982**, *23*, 234.

(3) Schue, F.; Aldissi, M.; Sledz, J.; Rolland, M.; Giral, L.; Dubois, J. C.; Gazard, M. *Colloq. Int. Nouv. Orientat. Composants Passifs: Mater. Technol. Misc. Deuvre [Commun.]* **1982**, 225; *Chem. Abstr.* **1983**, *99*, 158957w.

(4) Schue, F.; Aldissi, M.; Dubois, J. C.; Giral, L.; Rolland, M.; Sledz, J. *J. Phys. Colloq.* **1983**, *17*; *Chem. Abstr.* **1983**, *99*, 204146f.

(5) Theophilou, N.; Munardi, A.; Aznar, R.; Sledz, J.; Schue, F.; Naarmann, H. *Eur. Polym. J.* **1987**, *23*, 15.

(6) Voronkov, M. G.; Pukhnarevich, V. B.; Sushinskaya, S. P.; Annenkova, V. Z.; Annenkova, V. M.; Andreeva, N. J. *J. Polym. Sci., Polym. Chem. Ed.* **1980**, *18*, 53.

(7) Chien, J. C. W. *Polyacetylene, Chemistry, Physics and Material Sciences*; Academic Press: Orlando, FL, 1984.

(8) Munardi, A.; Theophilou, N.; Aznar, R.; Sledz, J.; Schue, F.; Naarmann, H. *Makromol. Chem.* **1987**, *188*, 395.

(9) Naarmann, H.; Theophilou, N. *Syn. Met.* **1987**, *22*, 1.

(10) Schimmel, T.; Riess, W.; Gmeiner, J.; Denninger, G.; Schwoerer, M.; Naarmann, H.; Theophilou, N. *Solid-State Commun.* **1988**, *65*, 1311.

(11) *Comprehensive Organometallic Chemistry*; Wilkinson, G., Stone, F. G. A., Abel, E. W., Hrsg.; Pergamon Press: Oxford, New York, Toronto, Sydney, Paris, Frankfurt, 1982; Vol. 3–6, 8.

(12) Otuska, S.; Nakamura, A. *Adv. Organomet. Chem.* **1976**, *14*, 245.

(13) Maitlis, P. M. *Acc. Chem. Res.* **1976**, *9*, 93.

(14) Maitlis, P. M. *J. Organomet. Chem.* **1980**, *200*, 161.

(15) Pörschke, K. R.; Tsay, Y.-H.; Krüger, C. *Angew. Chem.* **1985**, *97*, 334; *Angew. Chem., Int. Ed. Engl.* **1985**, *24*, 323.

(16) Hey, E.; Weller, F.; Dehnicke, K. *Naturwissenschaften* **1983**, *70*, 41.

(17) Hey, E.; Weller, F.; Dehnicke, K. *Z. Anorg. Chem.* **1984**, *514*, 18, 25.

(18) (a) Stahl, K.; Müller, U.; Dehnicke, K. *Z. Anorg. Chem.* **1985**, *527*, 7. (b) Stahl, K.; El-Kohli, A.; Müller, U.; Dehnicke, K. *J. Organomet. Chem.* **1986**, *316*, 95. (c) Stahl, K.; Weller, F.; Dehnicke, K. *Z. Anorg. Allg. Chem.* **1986**, *533*, 73.

(19) Kersting, M.; El.Kohli, A.; Müller, U.; Dehnicke, K. *Chem. Ber.* **1989**, *122*, 279.

(20) Neumann, P.; El.Kohli, A.; Müller, U.; Dehnicke, K. *Z. Anorg. Allg. Chem.* **1989**, *577*, 185.

(21) (a) Pauls, I.; Dehnicke, K.; Fenske, D. *Chem. Ber.* **1989**, *122*, 481. (b) Pauls, I. Dissertation, Universität Marburg, 1990.

(22) Kersting, M.; Dehnicke, K.; Fenske, D. *J. Organomet. Chem.* **1988**, *346*, 201.

0002-7863/93/1515-11930$04.00/0

evidence was found for the existence of vinylidene species in the case of molybdenum.[23]

In order to aid in investigating the reaction mechanism of the primary steps of the transition-metal-catalyzed acetylene polymerization, we studied the structures and stabilities of the transition-metal–alkyne and –vinylidene complexes using quantum mechanical ab initio methods. In recent systematic studies of the accuracy of effective core potentials (ECP) for calculating the geometries and energies of transition-metal compounds, we found[24] that the $(n-1)s^2\,(n-1)p^2\,(n-1)d^x\,(n)s^y$ ECP developed by Hay and Wadt[25] gives good results for closed-[24] and open-shell[26] transition-metal compounds if the (55/5/*N*) minimal basis set is split into (441/41/(*N*−1)1) or (441/2111/(*N*−1)1). This level of theory has successfully been used for studying the reaction mechanism of the cis-hydroxylation of olefins with OsO_4[27] and the structures and stabilities of the molecules $OsO_nF_{(8-2n)}$ (n = 0–4).[28] Here we report the results of the calculated structures for the alkyne and vinylidene complexes of tungsten and molybdenum halides. In order to investigate the electronic structure of the molecules, we used the natural bond orbital (NBO) partitioning scheme developed by Weinhold and co-workers.[29] We also employed the topological analysis of the wave function suggested by Bader and co-workers.[30]

Theoretical Details

All calculations were performed using the Convex and Fujitsu versions of GAUSSIAN90[31a] and GAUSSIAN92.[31b] Quasi-relativistic effective core potentials were used for molybdenum and tungsten.[25] The ECP valence basis sets for Mo and W were derived from the (55/5/4) basis set for Mo and (55/5/3) basis set for W optimized by Hay and Wadt.[25] The minimal basis sets were split into (441/2111/31) for Mo and (441/2111/21) for W (basis set I). For carbon, hydrogen, and fluorine, the standard 6-31G(d) basis functions[32a] were used. For the chlorine atom, the 3-21G(d) basis set[32b] was employed. We optimized the geometries of the complexes in the constraints of the respective point group at the Hartree–Fock (HF) level of theory using energy gradient techniques.[33] The harmonic vibrational frequencies were calculated using numerial second derivatives. All structures were verified as minima on the potential energy hyperface by only positive eigenvalues of the Hessian matrix. Improved total energies including correlation contributions were calculated using Møller–Plesset[34] perturbation theory terminated at second (MP2) or third (MP3) order in conjunction with the ECP valence basis set augmented by a set of f functions[35] (441/2111/(*N*−1)1/1) (basis set II). Unless otherwise noted, geometries are given at HF/I and energies at MP3/II. For the calculation of the electron density distribution $\rho(r)$, the gradient vector field $\nabla\rho(r)$, and its associated Laplacian $\nabla^2\rho(r)$, the programs PROAIM, SADDLE, GRID, and GRDVEC were used.[36]

Results and Discussion

In order to estimate the reliability of the theoretically predicted geometries, we optimized the octahedral structures WF_6, WCl_6, MoF_6, and $MoCl_6$. The geometries are shown in Table I; the calculated total energies are shown in Table II. The theoretically predicted bond lengths for WF_6, WCl_6, and MoF_6 are in good agreement with the experimental results. This is further evidence for our finding[24,27] that the geometries of transition-metal compounds in high-oxidation states can often be calculated with good accuracy at the Hartree–Fock level of theory.

As the next step in our investigation, we calculated the neutral complexes $WF_4C_2H_2$ (**1a**), $WCl_4C_2H_2$ (**1b**), $MoF_4C_2H_2$ (**2a**), and $MoCl_4C_2H_2$ (**2b**). The optimized structures are shown in Figure 2; the calculated geometries are listed in Table I.

There are no experimental geometries available which may be used to compare our results for structures **1a** and **2a**. Experimental data for **1b** and **2b** refer to dimeric complexes. They may be used to estimate the accuracy of the calculated bond lengths of the alkyne unit because it can be assumed that they are not strongly disturbed by the dimerization. Table I shows that the calculated M–C bond lengths are in good agreement with the experimental values for the dimeric structures. Note that the theoretical values refer to an ethyne ligand while the experimental values are taken from diphenylethyne complexes. This may be the reason for the difference between the theoretical and experimental values for the CC bond length. The ethyne ligand is predicted as having a stronger bend in the tungsten complexes **1a** and **1b** than in the molybdenum complexes **2a** and **2b**. This is in agreement with the experimentally observed trend (Table I). Also, the calculated C–C distances are longer in the tungsten complexes than in the Mo complexes, indicating stronger alkyne–metal interactions in **1a** and **1b** than in **2a** and **2b**. As shown below, the energy calculations predict higher bond energies for the W–C bonds than for the Mo–C bonds.

Why are chlorine complexes such as **1b** and **2b** in dimeric form stable but not the fluorine analogues **1a** and **2a**? We calculated the reaction energies for reactions 3–6 shown in Table III at the MP2 and MP3 levels using the (441/2111/(*N*−1)1/1) valence basis set. The absolute values for the calculated reaction energies should be used with some caution. Previous theoretical studies[37] have shown that the results at different orders of the MPn series sometimes show oscillating behavior. Better results may be obtained using coupled-cluster theory including single, double, and triple substitution (CCSD(T)).[38] However, we also found that the results at the MP2 level of theory are closed to the CCSD(T) values.[38b,c] In the present case, CCSD(T) calculations were not possible for us because the size of the investigated molecules is too large. But the theoretically predicted reaction energies at the MP2 and MP3 levels are sufficiently close to each other to allow a meaningful interpretation.

The results shown in Table III indicate that the formation of **1a** and **2a** from the corresponding metallahexafluorides and ethyne (reactions 3 and 4) is strongly endothermic by more than 100 kcal/mol. In contrast to the hexafluorides are the reactions of the metallahexachlorides with ethyne, yielding **1b** and **2b** nearly thermoneutral (reactions 5 and 6). This is in agreement with the experimental observation that neutral metallachloroalkyne com-

(23) Werth, A. Dissertation, Universität Marburg, 1992.
(24) Jonas, W.; Frenking, G.; Reetz, M. T. *J. Comput. Chem.* **1992**, *13*, 919.
(25) Hay, P. J.; Wadt, W. R. *J. Chem. Phys.* **1985**, *82*, 270, 284, 299.
(26) Veldkamp, A.; Frenking, G. *J. Comput. Chem.* **1992**, *13*, 1184.
(27) (a) Veldkamp, A., Frenking, G. *J. Am. Chem. Soc.*, submitted.
(28) Veldkamp, A.; Frenking, G. *Chem. Ber.* **1993**, *126*, 1325.
(29) (a) Forster, J. P., Weinhold, F. *J. Am. Chem. Soc.* **1980**, *102*, 7211. (b) Reed, A. E.; Weinstock, R. B.; Weinhold, F. *J. Chem. Phys.* **1983**, *78*, 4066. (c) Reed, A. E.; Weinstock, R. B.; Weinhold, F. *J. Chem. Phys.* **1985**, *83*, 735. (d) Reed, A. E.; Curtiss, L. A.; Weinhold, F. *Chem. Rev.* **1988**, *88*, 899. (e) Weinhold, F.; Carpenter, J. E. In *The Structure of Small Molecules and Ions*; Naaman, R., Vager, Z., Eds.; Plenum: New York, 1988; pp 227.
(30) (a) Bader, R. F. W. *Atoms in Molecules. A Quantum Theory*; Oxford Press: Oxford, 1990. (b) Bader, R. F. W.; Tal, Y.; Anderson, S. G.; Nguyen-Dang, T. T.; *Isr. J. Chem.* **1980**, *19*, 8. (c) Bader, R. F. W.; Nguyen-Dang, T. T.; Tal, Y. *Rep. Prog. Phys.* **1981**, *44*, 893. (d) Bader, R. F. W.; Nguyen-Dang, T. T. *Adv. Quantum Chem.* **1981**, *14*, 63. (e) Bader, R. F. W.; Slee, T. S.; Cremer, D.; Kraka, E. *J. Am. Chem. Soc.* **1983**, *105*, 5061. (f) Bader, R. F. W.; MacDougall, P. J. *J. Am. Chem. Soc.* **1985**, *107*, 6788.
(31) Frisch, M. J.; Head-Gordon, M.; Trucks, G. W.; Foresman, J. B.; Schlegel, H. B.; Raghavachari, K.; Robb, M. A.; Binkley, J. S.; Gonzales, C.; DeFrees, D. J.; Fox, D. J.; Whiteside, R. A.; Seeger, R.; Melius, C. F.; Baker, I.; Martin, R. L.; Kahn, L. R.; Stewart, J. J. P.; Topiol, S.; Pople, J. A. GAUSSIAN90; Gaussian Inc.: Pittsburgh, PA, 1990.
(32) (a) Ditchfield, R.; Hehre, W. J.; Pople, J. A. *J. Chem. Phys.* **1971**, *54*, 724. (b) Hehre, W. J.; Lathan, W. A. *J. Chem. Phys.* **1972**, *56*, 5255.
(33) Pulay, P. *Application of Electronic Structure Theory*; Schaefer, H. F., III. Ed.; Plenum Press: New York, 1977; p 153.
(34) (a) Møller, C.; Plesset, M. S. *Phys. Rev.* **1934**, *46*, 618. (b) Binkley, J. S.; Pople, J. A. *Int. J. Quantum Chem.* **1975**, *9*, 229.
(35) Ehlers, A.; Böhme, M.; Dapprich, S.; Gobbi, A.; Höllwarth, A.; Jonas, V.; Koehler, K. F.; Stegman, R.; Veldkamp, A.; Frenking, G. *Chem. Phys. Lett.* **1993**, *208*, 111.
(36) Biegler-König, F. W.; Bader, R. F. W.; Ting-Hua, T. *J. Comput. Chem.* **1982**, *3*, 317.
(37) (a) Marsden, C. J.; Wolynec, P. P. *Inorg. Chem.* **1991**, *30*, 1681. (b) Jonas, V.; Frenking, G.; Gauss, J. *Chem. Phys. Lett.* **1992**, 194, 109. (c) Neuhaus, A.; Frenking, G.; Huber, C.; Gauss, J. *Inorg. Chem.* **1992**, *31*, 5355.
(38) (a) Cizek, J. *J. Chem. Phys.* **1966**, *45*, 4256. (b) Pople, J. A.; Krishnan, R.; Schlegel, H. B.; Binkley, J. S. *Int. J. Quantum Chem.* **1978**, *14*, 545. (c) Bartlett, R. J.; Purvis, G. D. *Ibid.* **1978**, *14*, 561. (d) Purvis, G. D.; Bartlett, R. J. *J. Chem. Phys.* **1982**, *76*, 1910. (e) Raghavachari, K.; Trucks, G. W.; Pople, J. A.; Head-Gordon, M. *Chem. Phys. Lett.* **1989**, *157*, 479. (f) Bartlett, R. J.; Watts, J. D.; Kucharski, S. A.; Noga, J. *Ibid.* **1990**, *165*, 513.

Table I. Theoretically Predicted and Experimentally Observed Geometries of MX_6, C_2R_2, CCR_2, and the Alkyne and Vinylidene Complexes **1–10** (M = Mo, W; X = F, Cl; R = H, F)[a]

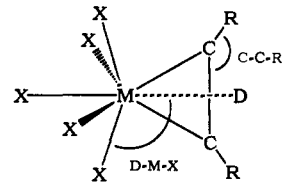

complex		M–C	C–C	C–M–C	C–R	C–C–R	M–X	D–M–X	ϑ[b]	ref
WF_6	O_h						1.815			49
							(1.830)			
WCl_6	O_h						2.303			50
							(2.32)			
MoF_6	O_h						1.812			51
							(1.82)			
$MoCl_6$	O_h						2.300			
HCCH	$D_{\infty h}$		1.186		1.057	180.0				
FCCF	$D_{\infty h}$		1.166		1.276	180.0				
CCH_2	C_{2v}		1.293		1.077	120.3				
CCF_2	C_{2v}		1.325		1.297	123.5				
1a	C_{2v}	1.995	1.294	37.9	1.070	145.0	1.862	105.1	45.0	
1b	C_{2v}	1.987	1.288	37.8	1.069	148.3	2.349	103.7	45.0	21b[e]
		(1.990)	(1.330)	(39.0)		(142.8)	(2.316)		(40.3)	
2a	C_{2v}	2.059	1.246	35.4	1.066	157.8	1.875	101.0	45.0[h]	
2b	C_{2v}	2.040	1.250	35.7	1.066	157.7	2.352	101.0	45.0[h]	
		(2.008)	(1.331)	(38.7)		(146.5)	(2.326)		(47.8)	21a[e]
3a	C_{2v}	2.051	1.275	36.2	1.069	146.7	1.901[d]	96.2[d]	45.0[h]	
		(2.036)	(1.210)	(34.5)			(1.892)	(96.9)	(36.5)	19[f]
							1.921[c]	180.0[c]		
							(1.991)	(179.3)		19[f]
3b	C_{2v}	2.048	1.261	35.9	1.064	153.2	2.425[d]	94.3[d]	45.0	
		(2.037)	(1.253)	(36.2)			(2.366)	(96.0)	(45.6)	21b[g]
							2.465[c]	180.0[c]		
							(2.490)	(178.6)		21b[g]
5	C_{2v}	1.990	1.302	38.2	1.285	142.3	1.852	105.6	45.0	
6	C_{2v}	1.975	1.280	37.8	1.276	147.6	1.861	103.4	45.0[h]	
7	C_{2v}	1.834	1.308		1.077	121.0	1.860	103.3	45.0[h]	
8	C_{2v}	1.793	1.325		1.274	124.6	1.851	104.8	45.0[h]	
9	C_{2v}	1.900	1.291		1.077	120.2	1.875	99.5	45.0[h]	
10	C_{2v}	1.785	1.328		1.270	123.9	1.861	103.1	45.0[h]	

[a] Bond distances A–B in Å, bond angles A–B–C in deg. Theoretical data are calculated at HF/I. The experimental data are given in parentheses. [b] ϑ represents the dihedral angle between the MCC and the MXX planes. A value of $\vartheta = 0$ indicates an eclipsed conformation; $\vartheta = 45$ indicates a staggered conformation. [c] Halogen ligand at trans position. [d] Halogen ligand at cis position. [e] Experimental values are given for the dimer with R = phenyl; X refers to the nonbridging Cl. [f] Experimental values are given for the anion with R = phenyl. [g] Experimental values are given for the anion with R = phenyl and R = H. [h] Energy minimum conformation at the MP2 and/or MP3 level, see text.

plexes (as dimers), but not metallafluoroalkyne complexes, are formed in reactions 3–6. This is because the M–F bonds are much stronger than the M–Cl bonds.

The optimized conformations of the complexes **2a** and **2b** calculated at the HF level of theory have the ethyne ligand eclipsing the M–halogen bonds. The energy differences calculated for the eclipsed and staggered conformations are very low, however. The staggered forms become more stable than the eclipsed forms when the correlation energy is calculated at the MP2 and MP3 levels. Different stability orders for the eclipsed and staggered conformations were also calculated at the HF and MPn levels of theory for the other alkyne and vinylidene complexes. Experimental results show that transition-metal alkyne complexes have mostly staggered conformations, although cases are known where the alkyne ligand is eclipsing the cis metal–ligand bond.[19] Because the calculated energy differences between the staggered and eclipsed conformations are low and may even change at different levels of theory, we do not think that it is justified to discuss them here.

Next in our investigation, we studied the anionic complexes $WF_5C_2H_2^-$ (**3a**), $WCl_5C_2H_2^-$ (**3b**), $MoF_5C_2H_2^-$ (**4a**), and $MoCl_5C_2H_2^-$ (**4b**). The optimized structures are shown in Figure 2. The results of an X-ray structure analysis for the tungsten complexes **3a** and **3b** are available and may be used for comparison with the calculated data. The metal carbon distance is theoretically predicted to be longer in the anionic complexes **3a** (2.051 Å) and **3b** (2.048 Å) than in the neutral structures **1a** (1.995 Å) and **1b** (1.987 Å). This is in agreement with the experimental results which show that the W–C distance in **3b** (2.037 Å) is longer than that in **1b** (1.990 Å).

The geometry optimizations of the molybdenum complexes **4a** and **4b** failed because the ethyne unit dissociates during the optimization procedure, giving C_2H_2 and the corresponding MoX_5^- fragment. It follows that **4a** and **4b** are not minima on the potential energy surface. This is in agreement with the experimental observation that in reaction 2 for M = Mo, only the halogen complexes $Mo_2X_{10}^{2-}$ could be isolated, whereas for M = W, structure **3a** or **3b** is formed (Figure 1).

We also investigated the influence of substituting hydrogen in the ethyne unit with fluorine. Figure 2 shows the optimized geometries of $WF_4C_2F_2$ (**5**) and $MoF_4C_2F_2$ (**6**). The calculated M–C distances in **5** (1.990 Å) and **6** (1.975 Å) are shorter than the corresponding M–C distances in **1a** (1.995 Å) and **2a** (2.059 Å) (Table I). Also, the C–C bonds in **5** (1.302 Å) and **6** (1.280 Å) are longer than those in **1a** and **1b**, although the C–C distance in FCCF is calculated to be shorter (1.166 Å, HF/I) than that in HCCH (1.186 Å). This indicates that difluoroacetylene may be more strongly bound in transition-metal complexes than ethyne. The calculated reaction energies for the isodesmic reactions 7 and 8 (Table III) are in agreement with this. C_2F_2 is theoretically predicted as being more strongly bound in **5** and **6** than C_2H_2 in **1a** and **2a**. Difluoroethyne complexes have recently been prepared,[39a] but there are no direct experimental data available for comparison with the predicted stronger binding of C_2F_2 over

Table II. Calculated Total Energies of Complexes **1–10** at the HF, MP2, and MP3 Levels of Theory (kcal/mol)

complex	state	total energies			
		basis set I	basis set II		
		HF	HF	MP2	MP3
F_2	$^1\Sigma_g^+$	−198.67346	−198.67346	−199.02525	−199.02488
Cl_2	$^1\Sigma_g^+$	−918.90930	−918.90930	−919.16406	−919.18946
C_2H_2	$^1\Sigma_g^+$	−76.81732	−76.81732	−77.06142	−77.07245
C_2F_2	$^1\Sigma_g^+$	−274.45680	−274.45680	−275.03107	−275.03177
CCH_2	$^1A_1$	−76.76287	−76.76287	−76.98167	−77.00408
CCF_2	$^1A_1$	−274.42662	−274.42668	−274.97293	−274.98598
WF_6	$^1A_{1g}$	−663.95847	−664.00935	−665.43104	−665.35493
WCl_6	$^1A_{1g}$	−2824.07925	−2824.10963	−2825.30677	−2825.27550
MoF_6	$^1A_{1g}$	−663.50510	−663.55218	−665.07806	−664.96455
$MoCl_6$	$^1A_{1g}$	−2823.68962	−2823.71037	−2825.02508	−2824.92857
1a	$^1A_1$	−541.88120	−541.91574	−543.22362	−543.17526
1b	$^1A_1$	−1982.01490	−1982.03819	−1983.17776	−1983.16901
2a	$^1A_1$	−541.50471	−541.53067	−542.89738	−542.84056
2b	$^1A_1$	−1981.67066	−1981.68645	−1982.89332	−1982.86743
3a	$^1A_1$	−641.41970	−641.45463	−642.94395	−642.89890
3b	$^1A_1$	−2441.61350	−2441.63554	−2442.91644	−2442.92141
5	$^1A_1$	−739.54280	−739.58025	−741.23276	−741.16586
6	$^1A_1$	−739.15129	−739.18200	−740.92814	−740.83075
7	$^1A_1$	−541.85961	−541.89056	−543.19940	−543.15201
8	$^1A_1$	−739.55970	−739.59351	−741.24907	−741.17731
9	$^1A_1$	−541.48775	−541.51213	−542.86131	−542.81303
10	$^1A_1$	−739.17112	−739.19961	−740.93619	−740.84365

C_2H_2. It should be noted that difluoroethylene is known to be more strongly bound in transition-metal complexes than ethylene.[39b,c]

Next in our investigation, we calculated the structures and the relative energies of vinylidene isomers. The optimized geometries of the vinylidene and difluorovinylidene complexes **7–10** are shown in Figure 2. Table I shows that the M–C bonds are predicted to be significantly shorter in the vinylidene complexes **7–10** than in the corresponding acetylene complexes **1a**, **5**, **2a**, and **6**. Experimentally derived geometries for tungsten and molybdenum vinylidene complexes are available but only for the low-oxidation states of W and Mo. Typical M–CCR_2 bond distances for M = W, Mo are in the range 1.90–2.00 Å.[40] The C–C bond lengths in these complexes are 1.30–1.38 Å.[40] The M–C distances calculated for **7**, **8**, and **10** are clearly shorter than the observed values.[40] Interestingly, structure **9** has a significantly longer Mo–C bond (1.900 Å) as compared to the W–C bond in **7** (1.834 Å) while the Mo–C and W–C bonds in the difluorovinylidene complexes **8** and **10** have nearly the same value (Mo–C = 1.785 Å and W–C = 1.793 Å). As discussed below, this is caused by the different polarity of the M–C π bond, which is nearly symmetrical in **7** but strongly polarized toward the metal atom in **9**. The C–C bond of the vinylidene ligand in **7** (1.308 Å) is calculated as being longer than that in the isolated vinylidene (1.293 Å), whereas the C–C bond length in **9** (1.291 Å) has hardly changed upon complexation (Table I). The C–C distances in the difluorovinylidene complexes **8** (1.325 Å) and **10** (1.328 Å) are nearly the same as those in the isolated ligand (1.325 Å). The metal–carbon distances in the difluoro complexes **8** and **10** are clearly shorter than those in the dihydrogen complexes **7** and **9**. This indicates that the difluorovinylidene ligand may be more strongly bound than the vinylidene ligand, similar to that calculated for the ethyne isomers. The calculated energies for the isodesmic reactions 9 and 10 also predict that the difluorovinylidene ligands in **8** and **10** are more strongly bound than the vinylidene in **7** and **9** (Table III).

What are the relative energies of the alkyne and vinylidene isomers? Table IV shows that the calculated energy differences do not change much at different levels of theory. At MP3/II, the ethyne isomer **1a** is 14.6 kcal/mol lower in energy than the vinylidene structure **7**. In case of molybdenum, the ethyne structure **2a** is 17.3 kcal/mol lower in energy than the vinylidene

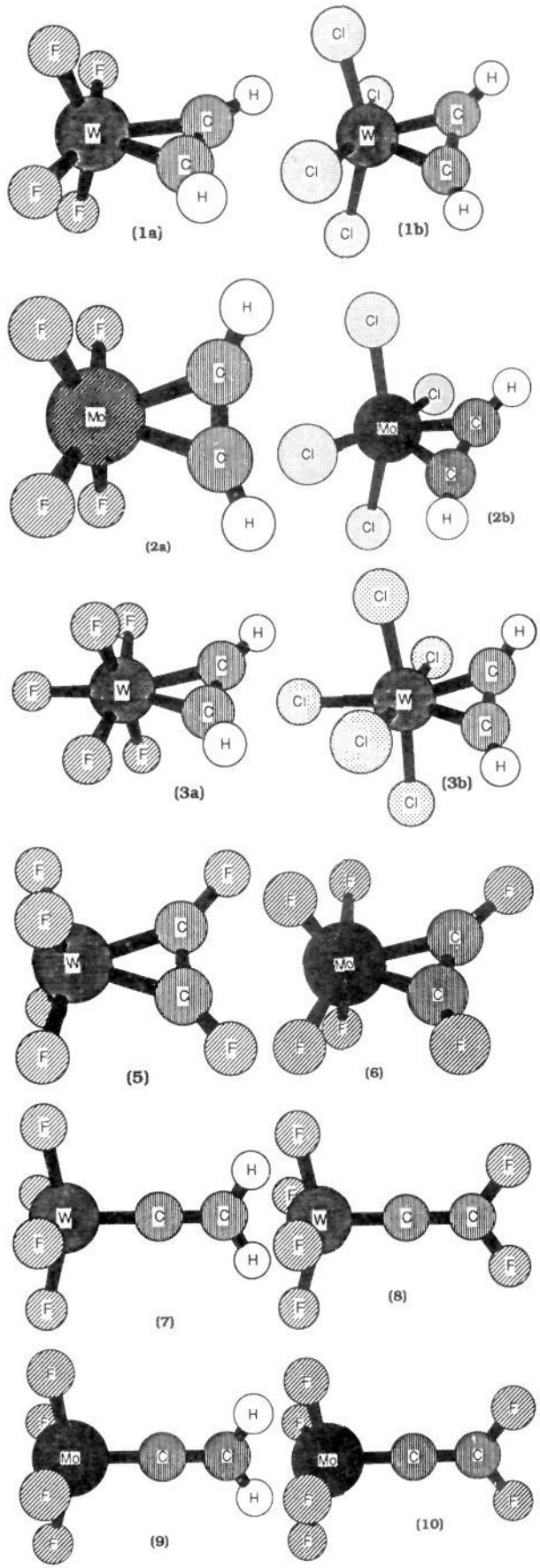

Figure 2. Optimized structures (HF/I) of the complexes **1a–10**.

(39) Lentz, D.; Michael, H. *Angew. Chem.* **1988**, 100, 871; *Angew. Chem., Int. Ed. Engl.* **1988**, 27, 845. (b) Cramer, R. *J. Am. Chem. Soc.* **1967**, 89, 4621. (c) Cramer, R.; Parshall, G. *J. Am. Chem. Soc.* **1965**, 87, 1392.

(40) Bruce, M. I. *Chem. Rev.* **1991**, *91*, 197.

Table III. Reaction Energies ΔE for Reactions 3–10 at the MP2 and MP3 Levels of Theory Using Basis Set II (kcal/mol)[a]

educts		products	ΔE	no.
$WF_6 + C_2H_2$	→	$WF_4C_2H_2 + F_2$	+152.9	3
		1a	+142.6	
$MoF_6 + C_2H_2$	→	$MoF_4C_2H_2 + F_2$	+136.1	4
		2a	+107.7	
$WCl_6 + C_2H_2$	→	$WCl_4C_2H_2 + Cl_2$	+16.5	5
		1b	−6.6	
$MoCl_6 + C_2H_6$	→	$MoCl_4C_2H_2 + Cl_2$	+18.3	6
		2b	−35.1	
$WF_4C_2H_2 + C_2F_2$	→	$WF_4C_2F_2 + C_2H_2$	−24.8	7
1a		**5**	−19.6	
$MoF_4C_2H_2 + C_2F_2$	→	$MoF_4C_2F_2 + C_2H_2$	−38.3	8
2a		**6**	−19.4	
$WF_4CCH_2 + CCF_2$	→	$WF_4CCF_2 + CCH_2$	−36.7	9
7		**8**	−27.2	
$MoF_4CCH_2 + CCF_2$	→	$MoF_4CCF_2 + CCH_2$	−52.5	10
9		**10**	−30.6	

[a] First value MP2, second value MP3.

Table IV. Calculated Relative Energies of Complexes **1a**, **2a**, **5**, **6**, **7**, **8**, **9**, and **10** at the HF, MP2, and MP3 Levels of Theory (kcal/mol)

	relative energies			
	basis set I	basis set II		
complex	HF	HF	MP2	MP3
1a	0	0	0	0
7	13.5	15.8	15.2	14.6
2a	0	0	0	0
9	10.6	11.6	22.6	17.3
5	0	0	0	0
8	−10.6	−8.3	−10.2	−7.2
6	0	0	0	0
10	−12.4	−11.1	−5.1	−8.1

isomer **9**. Substitution of hydrogen by fluorine changes the relative stability. The difluorovinylidene isomers **8** and **10** are clearly lower in energy than the corresponding complexes **5** and **6** (Table IV). This means that substitution of hydrogen by fluorine is theoretically predicted to give a higher stability to the vinylidene isomers in transition-metal complexes relative to the corresponding alkyne isomers.

Figure 3 shows the most important orbital interactions for the alkyne and vinylidene complexes using the Dewar, Chatt, and Duncanson model.[41] The metal–alkyne bonding is explained by electron donation from the occupied π MO (HOMO) of the alkyne ligand into the empty d_{z^2} AO of the metal (Figure 3a) and back-donation from the d_{zy} (M) AO into the π^* LUMO of the alkyne (Figure 3b). Similarly, the metal–vinylidene bonding is rationalized in terms of electron donation from the lone pair HOMO of the vinylidene into the d_{z^2} AO of the metal (Figure 3c) and back-donation from the d_{zy} (M) AO into the π^* LUMO of the vinylidene (Figure 3d). In the following, we will investigate the electronic structure of the alkyne and vinylidene complexes **1–10** quantitatively using the NBO population scheme[29] and the topological analysis of the wave function.[30] Of particular interest are the oxidation states of tungsten and molybdenum and the nature of the M–C bonds in these complexes. If ethyne and vinylidene are four-electron donors, the oxidation state would be M(+VI). In this case, **1–10** would be formal d(0) complexes. If ethyne and vinylidene donate only two electrons, the oxidation state would be M(+IV). Then, molecules **1–10** would be d(2) complexes. The results of magnetic susceptibility measurements of the analogous rhenium alkyne complexes $[ReCl_4(PhCCPh)_2]$ reported by Swidersky et al.[42] indicate a d(1) configuration for rhenium corresponding to an oxidation state of Re(+VI). A recently reported experimental and theoretical study of tungsten

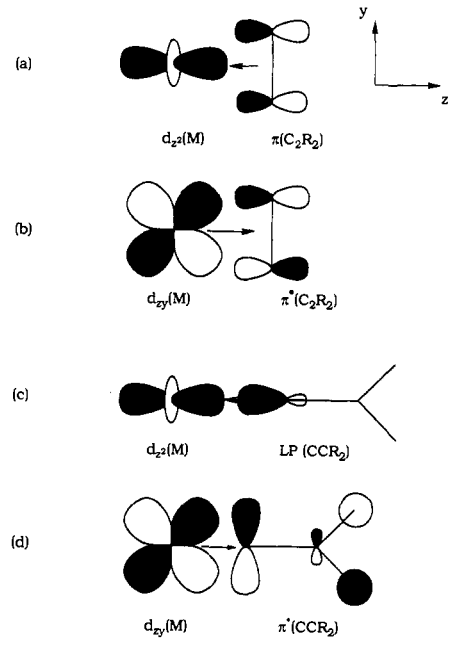

Figure 3. Schematic representation of the most important orbital interactions between the C_2H_2 ligand and the metal: (a) alkyne → metal donation, (b) metal → alkyne back-donation, (c) vinylidene → metal donation, and (d) metal → vinylidene back-donation.

alkyne complexes suggests an oxidation state of W(+VI) in these compounds.[43]

Table V shows the results of the NBO analysis for **1–10**. The NBO data[a] for the metal hexahalogens MX_6 are shown for comparison. The occupation of the $(n-1)$d orbital in W and Mo in the hexafluorides is 2.09 e in WF_6 and 2.44 e in MoF_6. The occupation of the (n)s orbital is very low, 0.26 e in WF_6 and 0.23 e in MoF_6. The partial charges in MF_6 are +3.57 for W and +3.23 for Mo. The occupation of the metal $(n-1)$d orbitals in the ethyne complexes **1a** and **2a** is slightly higher, 2.83 e in **1a** and 3.26 e in **2a**. Accordingly, the positive charges at the metal atoms are slightly reduced, +2.83 for W in **1a** and +2.43 for Mo in **2a**. The metal (n)s occupation in the alkyne complexes remains low.

Similar results are calculated for the chlorine complexes **1b** and **2b**. However, the occupation of the metal $(n-1)$d orbitals in **1b** and **2b** is *lower* than that in the metal hexachlorides (Table V). There are 4.36 e in the 5d orbital of W in WCl_6 but only 4.09 e in that of **1b**. In $MoCl_6$ there are 4.73 e in the 4d orbital of Mo but only 4.44 e in that of **2b**. Accordingly, the partial charges at the metals are slightly more positive in **1b** and **2b** than in the corresponding hexachlorides (Table V). The occupation of the 5d AO of W and the partial charge at tungsten in the anionic complexes **3a** and **3b** are very similar to those in the analogous neutral complexes **1a** and **1b**. The fluoroethyne complexes **5** and **6** have metal AO occupations which are nearly the same as those in the analogous ethyne complexes **1a** and **2a**. The main difference is the partial charge at the carbon atoms. The carbon atoms of the ethyne complexes **1a** and **2a** carry a positive charge, while the carbon atoms of the fluoroethyne complexes **5** and **6** have a negative charge. The calculated metal AO populations and the partial charges at the metal atoms demonstrate a large difference between the formal atomic populations and the oxidation states. WCl_6 and $MoCl_6$ are classified as d(0) compounds with the oxidation state +VI, but the NBO analysis shows only a partial charge +1.04 at W and +0.78 at Mo. The most important result of the NBO analysis is that the positive charges at the metals are *higher* in the ethyne complexes **1b**, **2b**, and **3b** than in the respective hexachloride.

(41) (a) Dewar, M. J. S. *Bull. Soc. Chim. Fr.* **1951**, *18*, C71. (b) Chatt, J.; Duncanson, L. A. *J. Chem. Soc.* **1953**, 2939.

(42) Swidersky, H.-W.; Pebler, J.; Dehnicke, K.; Fenske, D. *Z. Naturforsch.* **1980**, *45b*, 1227.

(43) Nielson, A. J.; Boyd, P. D. W.; Clark, G. R.; Hunt, T. A.; Metson, J. B.; Rickhard, C. E. F.; Schwerdtfeger, P. *Polyhedron* **1992**, *11*, 1419.

Table V. Results of the NBO Analysis

	metal AO population[a]			M–C bond[a,b]					charges		
	(*n*)s	(*n*-1)d	(*n*)p	pop.[c]	% M	% (*n*)s	% (*n*)p	% (*n*-1)d	q_M	q_C	q_X
1a	0.26	2.83	0.02	1.91 (0.17)	36.0	12.6	0.3	87.1	2.83	–0.42	–0.63
1b	0.39	4.09	0.02	1.80 (0.20)	37.9	17.4	7.7	74.9	1.39	–0.30	–0.34
2a	0.20	3.26	0.01	1.81 (0.27)	48.8	8.0	0.3	91.7	2.43	–0.26	–0.62
2b	0.30	4.44	0.00	1.71 (0.29)	49.0	20.7	1.0	78.4	1.13	–0.19	–0.34
3a	0.25	2.79	0.02	1.86 (0.25)	34.7	13.0	0.3	86.7	2.82	–0.45	–0.67
											–0.68[e]
3b	0.39	4.21	0.02	1.78 (0.36)	43.8	23.8	1.4	74.8	1.22	–0.31	–0.42
											–0.47[e]
5	0.28	2.86	0.01	1.92 (0.17)	33.6	12.3	0.4	87.3	2.80	0.17	–0.62
6	0.23	3.27	0.00	1.90 (0.21)	41.8	7.8	0.3	91.8	2.42	0.30	–0.59
7	0.28	2.92	0.02	σ 1.99 (0.12)	27.4	17.6	0.1	82.3	2.76	–0.46	–0.63
				π 1.98 (0.12)	59.3	0.0	0.7	99.3		–0.26[d]	
8	0.28	2.83	0.02	σ 1.99 (0.13)	29.0	17.2	0.1	82.8	2.85	–0.82	–0.62
				π 1.95 (0.13)	46.2	0.0	0.7	99.3		1.14[d]	
9	0.23	3.34	0.02	σ 1.97 (0.08)	23.7	35.3	0.1	64.6	2.37	–0.03	–0.63
				π 1.63 (0.09)	76.9	0.0	24.6	75.4		–0.38[d]	
10	0.00[f]	3.25	0.00	σ 1.99 (0.15)	30.9	12.1	0.1	87.9	2.45	–0.50	–0.60
				π 1.97 (0.11)	61.2	0.0	0.3	99.7		1.11[d]	
WF_6	0.26	2.09	0.03						3.57		–0.59
WCl_6	0.45	4.36	0.09						1.04		–0.17
MoF_6	0.23	2.44	0.00						3.23		–0.54
$MoCl_6$	0.36	4.73	0.00						0.78		–0.13

[a] $n = 5$ for Mo; $n = 6$ for W. [b] Pop. represents the population of the M–C bond, % M gives the contribution of the M–C bond at atom M and %(*n*)s, %(*n*)p, and %(*n*–1)d give the hybridization of the M–C bond at M. [c] The first value gives the population of the M–C bond. The population of the corresponding M–C antibond is given in parentheses. [d] For the vinylidene complexes **7**–**10**, the first carbon atom is C_α and the second is C_β. [e] These values refer to the halogen ligand at trans position. [f] 6s: 0.24.

This means that ethyne is a better acceptor ligand than two chlorine atoms. Alternatively, $HCCH^{2-}$ is a poorer donor than two Cl^-. In any case, the ethyne ligand should formally be considered as a $HCCH^{2-}$ ligand acting as a four-electron donor. The alkyne complexes **1**–**6** should be classified as d(0) complexes with the formal oxidation state +VI at the metal. This is in agreement with previous studies.[42,43]

What about the vinylidene complexes **7**–**10**? Table V shows that the occupation of the metal (n – 1)d orbitals and the (n)s orbital and the partial charge at the metals in the vinylidene complexes **7**–**10** are very similar to those of the corresponding alkyne complexes **1a**, **2a**, **5**, and **6**. Vinylidene is a slightly better donor (weaker acceptor) than ethyne, as shown by the higher occupation of the metal (n – 1)d orbital in **7** and **9** than in **1a** and **2a**. Thus, the NBO analysis suggests that the ethyne and vinylidene complexes **1**–**10** have the oxidation state M(+VI).

The M–C bonds need to be analyzed in more detail. Table V shows that the M–C bonding orbitals of the alkyne complexes **1**–**6** are occupied by 1.65–1.89 e. The M–C bonding is somewhat reduced by partial occupation of the M–C antibonding orbital with 0.14–0.36 e. The occupancy of the bonding orbital is higher for the W–C bond in **1a** and **1b** than for the Mo–C bonds in **2a** and **2b** and the W–C bonds in **3a** and **3b**. It is also higher for the M–C bonds in the fluoroethyne complexes **5** and **6** than for those in the ethyne complexes **1a** and **2a**, which agrees with the calculated stronger bonds of the former complexes. The M–C bonds are always polarized toward the carbon end as shown by the % M values (Table V). The M–C bonds are more polarized toward C in the tungsten complexes than in the corresponding molybdenum complex, and they are more strongly polarized in the fluoro complexes than in the corresponding chloro complexes. As expected, the hybridization of the M–C bond at the metal shows dominantly (n – 1)d character.

Two M–C bonds were analyzed by the NBO partition scheme for the vinylidene complexes **7**–**10**, one σ and one π bond. The σ bond is always strongly polarized toward the carbon end while the polarization of the π bond depends upon the metal and the electronegativity of the ligand. In the vinylidene complex **7**, the W–C π bond is slightly polarized toward tungsten, but it is clearly polarized toward the carbon end in the difluorovinylidene complex **8** (Table V). For the molybdenum complexes **9** and **10**, the polarity is significantly shifted toward the metal atom. The most intriguing result is the big difference in the polarization of the W–C and Mo–C π bonds in the vinylidene complexes **7** and **9**. The W–C π bond in **7** is nearly symmetrical (59.3% at W), but the Mo–C π bond in **9** is strongly polarized toward molybdenum (76.9% at Mo). This explains the difference in the calculated partial charges at C_α and C_β in **7** and **9**. In the tungsten complex **7**, C_α carries a larger negative partial charge (–0.46 e) than C_β (–0.26 e). The opposite result is calculated for the molybdenum complex **9**. Here, the negative charge at C_α is much lower (–0.03 e) than that at C_β (–0.38 e). Thus, the polarity of the M–C π bond and, subsequently, the charge distribution at C_α and C_β of the vinylidene ligand are strongly dependent upon the metal atom. It should also be noted that in the difluorovinylidene complexes **8** and **10**, the charge polarity at the ligand is very large. The C_β atoms carry a positive charge of >+1.0, and the C_α atoms are negatively charged with –0.82 e (**8**) and –0.50 e (**10**).

In a previous molecular orbital study of the electronic structure of vinylidene complexes by Kostic and Fenske,[44] it was shown that nucleophilic attack on a vinylidene ligand in transition-metal complexes should occur at C_α and electrophilic attack at C_β. But it was also shown that the partial charges at the carbon atoms may change significantly with different transition metals and that C_α or C_β may be the most negative ligand atom.[44] It seems possible that charge and orbital factors may both influence the nucleophilic attack of a vinylidene ligand as suggested already by Kostic and Fenske[44] for the electrophilic attack. We want to point out that the frontier orbitals calculated for the vinylidene complexes **7**–**10** show the opposite order as predicted by approximate Fenske–Hall-type calculations for cyclopentadienylcarbonyl complexes of manganese.[44] The HOMO in **7**–**10** is mainly the bonding combination of the d_{zy} metal orbital and the C–C π^* in-plane orbital (zy being the molecular plane of the vinylidene fragment) as schematically shown in Figure 3b. The largest coefficient is at the metal d_{zy} AO, but the coefficient at C_α is always larger than that at C_β. The LUMO in **7**–**10** is mainly the antibonding combination of the d_{zy} metal AO and the C–C π^* orbital of vinylidene. Again, the largest coefficient is at the metal (d_{zy}) AO, but the coefficient at C_β is now larger than that at C_α. The frequently observed[40] protonation of electron-poor vinylidene complexes at C_β appears to be controlled by the charge distribution at the carbon atoms. Because the charges at

(44) Kostic, N. M.; Fenske, R. F. *Organometallics* **1982**, *1*, 974.

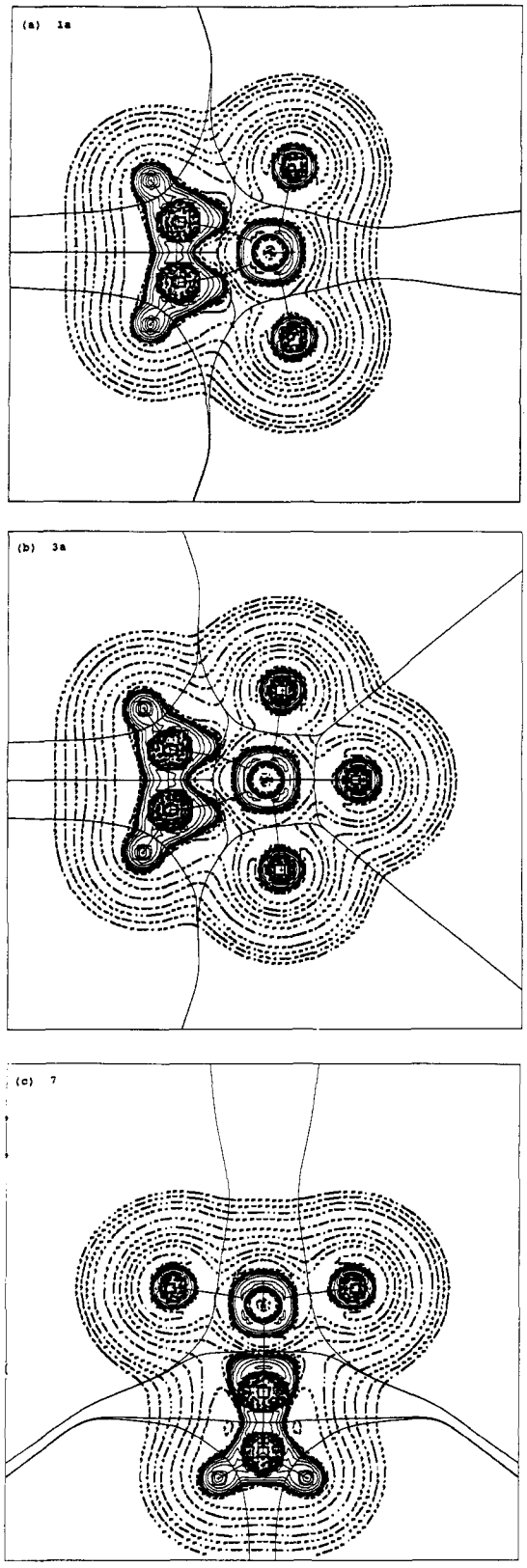

Figure 4. Contour line diagrams of the Laplacian distribution $\nabla^2\rho(r)$ of **1a** (a), **3a** (b), and **7** (c).[52] Dashed lines indicate charge depletion ($\nabla^2\rho(r) > 0$); solid lines indicate charge concentration ($\nabla^2\rho(r) < 0$). The solid lines connecting the atomic nuclei are the bond paths, the solid lines separating the atomic nuclei indicate the zero-flux surfaces in the molecular plane, and the crossing points are the critical points.

C_α and C_β are calculated to be strongly dependent upon the polarity of the M–C π bond, the different products which are found upon protonation of vinylidene complexes[40] may be caused by the effect of the ligands upon the M–C π polarity. We will investigate this in a future study.

The results of the topological analysis of the electronic structures for the acetylene and vinylidene complexes **1–10** are shown in Table VI. The Laplacian distribution $\nabla^2\rho(r)$ for the complexes **1a**, **3a**, and **7** (Figure 5) shows regions of electron depletion ($\nabla^2\rho(r) > 0$, dashed lines) and electron concentration ($\nabla^2\rho(r) < 0$, solid lines). The solid lines connecting the atomic nuclei are the bond paths. The solid lines separating the nuclei indicate the zero-flux surfaces in the molecular plane. The points where the solid lines are crossing between the atoms are the bond critical points r_b.[30,52]

The contour line diagram for the acetylene complex **1a** depicted in Figure 4a shows that the tungsten and fluorine atoms possess a nearly spherical electron distribution as revealed by the shape of the Laplacian distribution. This indicates that the W–F bonds are largely ionic. The carbon atoms, however, exhibit a strongly anisotropic Laplacian distribution with an area of electron concentration ($\nabla^2\rho(r) < 0$, solid lines) pointing toward tungsten, which is typical for a semipolar bond. All alkyne complexes **1a–6** investigated in this study show electron density gradients and zero-flux surfaces which are typical for cyclic structures, i.e., they possess two M–C bond critical points r_b and one ring critical point.[30] The shape of the Laplacian distribution indicates a more covalent character for the W–C bond than for the W–F bond. This is supported by the calculated energy density at the bond critical point H_b. Systematic studies[45] have shown that a necessary and sufficient condition for a covalent bond is a negative value for H_b, with typical values for strong covalent bonds between –1 and –3. Table VI shows that H_b for the C–C and C–H bonds of **1a** is –3.14 and –2.11, respectively. The W–C bond of **1a** has a value of $H_b = -0.56$ while the W–F bonds have a H_b value of –0.20.

The shapes of the Laplacian distributions for **1b**, **2a**, and **2b** are very similar to **1a** and, therefore, are not shown here. The H_b values listed in Table VI show that the M–C bonds are slightly more covalent in the chlorine complexes **1b** and **2b** than in the corresponding fluorine complexes **1a** and **2a**. More important, however, are the differences between the tungsten complexes **1** and the molybdenum complexes **2**. The latter show a higher covalency for the C–C bonds and a lower covalency for the M–C bonds than the former as revealed by the H_b values (Table VI). This is in agreement with the calculated bond distances, which predict shorter C–C and longer M–C bonds for **2a** and **2b** than for **1a** and **1b** (Table I).

The shape of the Laplacian distribution for the anionic complex **3a** (Figure 5b) is very similar to that for **1a** (Figure 5a). The W–C bonds of **3a** and **3b** have an energy density at the bond critical point of $H_b = -0.43$ (**3a**) and $H_b = -0.45$ (**3b**). This is less than what is calculated for the W–C bonds in the neutral complexes **1a** and **1b**. It indicates that the W–C bonds in **3a** and **3b** are less covalent than those in the neutral complexes. Because the breaking of the W–C bonds yields neutral C_2H_2, the lower covalency points toward weaker W–C binding in **3a** and **3b** than in **1a** and **1b**. The H_b values for the Mo–C bonds of the neutral molybdenum complexes **2a** and **2b** are even lower than the H_b values for the W–C bonds in **3a** and **3b**. Since the addition of a halogen anion yields less covalent (weaker) M–C bonds, it becomes understandable that the anionic complexes $MoF_5C_2H_2^-$ (**4a**) and $MoCl_5C_2H_2^-$ (**4b**) are not minima on the potential energy surface. The Mo–C interactions in **4a** and **4b** are too weak, and therefore, C_2H_2 dissociates upon addition of X^- to **2a** or **2b**.

The H_b values for the M–C bonds of the difluoroacetylene complexes **5** and **6** indicate a covalent character comparable to those for the W–C bonds in **1a** and **2a** (Table VI). This means that the Mo–C bonds in **6** ($H_b = -0.57$) are more covalent (and stronger) than those in **2a** ($H_b = -0.41$). As expected, a stronger covalent character is also predicted for the M–C (double) bond in the vinylidene complexes **7–10** than for the M–C bonds in the

(45) Cremer, D.; Kraka, E. *Angew. Chem.* **1984**, *96*, 612; *Angew. Chem., Int. Ed. Engl.* **1984**, *23*, 627.

Table VI. Electron Density ρ_b (e/Å^3), $\nabla^2\rho_b$ (e/Å^5), and Energy Density H_b (hartree/Å^3) at the Bond Critical Points r_b and Shift of the Bond Critical Point Δr_b (Å) Relative to the Nonpolar Midpoint of Complexes **1–10**

	1a	**1b**	**2a**	**2b**	**3a**	**3b**	**5**	**6**	**7**	**8**	**9**	**10**
M–C												
ρ_b	1.05	1.06	0.90	0.91	0.92	0.93	1.05	1.09	1.34	1.44	1.13	1.44
$\nabla^2\rho_b$	1.75	1.99	2.44	3.00	2.39	2.46	2.93	2.57	8.23	7.42	10.02	8.14
H_b	–0.56	–0.57	–0.41	–0.41	–0.43	–0.45	–0.56	–0.57	–0.87	–1.01	–0.56	–0.95
Δr_b	0.17	0.19	0.20	0.20	0.17	0.19	0.16	0.18	0.15	0.16	0.14	0.17
C–C[a]												
ρ_b	2.50	2.53	2.67	2.66	2.53	2.60	2.50	2.54	2.48	2.35	2.59	2.39
$\nabla^2\rho_b$	–27.64	–27.98	–30.14	–30.31	–27.40	–28.65	–28.59	–28.65	–30.20	–20.38	–33.92	–25.89
H_b	–3.14	–3.20	–3.63	–3.60	–3.25	–3.43	–3.10	–3.24	–3.03	–3.89	–3.54	–3.95
Δr_b	0.00	0.00	0.00	0.00	0.00	0.00	0.00	0.00	0.00	–0.21	0.07	–0.20
C–R												
ρ_b	1.94	1.95	1.96	1.97	1.92	1.97	1.96	2.03	1.95	2.10	1.91	2.13
$\nabla^2\rho_b$	–27.85	–29.03	–29.99	–30.71	–26.32	–29.03	16.78	16.88	–27.37	11.78	–26.93	12.18
H_b	–2.11	–2.18	–2.24	–2.28	–2.05	–2.20	–2.68	–2.81	–2.10	–3.05	–2.06	–3.11
M–L												
ρ_b	0.99	0.60	0.95	0.58	0.88	0.50	1.02	0.99	0.99	1.01	0.94	0.99
$\nabla^2\rho_b$	20.62	4.39	20.12	4.83	18.34	3.85	21.10	20.47	21.01	21.31	20.36	20.67
H_b	–0.20	–0.14	–0.15	–0.12	–0.12	–0.10	–0.22	–0.19	–0.19	–0.21	–0.14	–0.18
Δr_b	0.38	0.54	0.39	0.54	0.38	0.54	0.38	0.38	0.38	0.38	0.38	0.38
M–L[b]												
ρ_b					0.84	0.45						
$\nabla^2\rho_b$					18.19	4.26						
H_b					–0.10	–0.10						
Δr_b					0.39	0.54						

[a] For the vinylidene complexes **7–10**, the first carbon atom is C_α and the second is C_β. [b] These values refer to the halogen ligand at trans position.

corresponding alkyne complexes (compare the H_b values for the M–C bonds of **1a** with **7**, **2a** with **9**, **5** with **8**, and **6** with **10** in Table VI). The fluorovinylidene complexes **8** and **10** have more covalent (and stronger) M–C bonds than the vinylidene complexes **7** and **9**.

The location of the bond critical point r_b between two atoms A and B reveals helpful information about the bond A–B. The shift of r_b from the "nonpolar" midpoint of bond A–B may be used as a measure for the effective electronegativity of the atoms.[47] If A and B are identical, the midpoint is simply half of the calculated interatomic distance. If A and B are different as in the case of the M–X (M = W, Mo) bonds, the sum of the ionic radii[48] a_M and a_X, corrected by the actual interatomic distance r_{MX}, may be used to define the nonpolar midpoint of the M–X bond m_{MX}. If the latter is given by the distance to the metal atom m_M, we define m_M as:

$$m_M = a_M r_{MX}(a_M + a_X)^{-1}$$

m_M = distance of the nonpolar midpoint from M

a_M = ionic radius of M^{6+}

a_X = ionic radius of X (X = Cl^-, F^-, C)

r_{MX} = calculated interatomic distance M–X

The shift in the bond critical point Δr_b is then given by the distance between r_b and m_M for the M–X bond, with negative (positive) values indicating that r_b is shifted toward the M (X) atom. The same method can be applied to the C–C bond, which is polarized toward one carbon atom in the case of the vinylidene complexes **7–10**.

The results in Table VI show clearly that the bond critical point r_b for the M–C bond is always significantly shifted toward the carbon atom. The position of the bond critical point r_b suggests that the electronegativity of M^{6+} is *higher*[46] than that of carbon, which is in agreement with chemical intuition. The shift of the critical point Δr_b is nearly the same (0.16–0.20 Å) for the tungsten and molybdenum alkyne complexes **1–6**. Slightly smaller values are calculated for the vinylidene complexes **7–10** (0.14–0.17 Å), which indicate that the C_α of vinylidene is more electronegative than the ethyne carbon atom. The C–C bond of the vinylidene complexes **7** and **9** is only weakly polarized (Δr_b = –0.00 Å for **7** and Δr_b = 0.07 Å for **9**), but it is clearly polarized in the fluoro complexes **8** and **10** (Δr_b = –0.21 Å for **8** and Δr_b = –0.20 Å for **10**). This demonstrates that the location of the bond critical point r_b is a very sensitive probe for the polarity and the effective electronegativity of the bonded atoms.

The M–L (L = Cl, F) bonds show larger differences for the shift of the bond critical point Δr_b than the M–C bonds (Table VI). The Mo–F and W–F bonds have nearly the same Δr_b values (0.38–0.39 Å). The W–Cl bonds are more polarized than the W–F bonds.

Summary

The optimized geometries of the chlorine and fluorine acetylene complexes of tungsten and molybdenum are in good agreement with experimental values for neutral and anionic molecules. The theoretical data indicate that the alkyne ligand is more strongly bound in the tungsten complexes than in the molybdenum complexes and that it is more strongly bound in fluoro complexes than in chloro complexes. The optimized geometries of the anionic tungsten complexes **3a** and **3b** have significantly longer W–C bond lengths than those of the neutral complexes **1a** and **1b**. The

(46) The bond critical point r_b is the crossing point of the zero-flux surface and the bond path.[30] The location of r_b of bond A–B is shifted toward A and, thus, assigns a larger area of the electronic charge to B if B is more electronegative than A.

(47) Otto, M.; Lotz, S. D.; Frenking, G. *Inorg. Chem.* **1992**, *31*, 3647.

(48) The following values for the ionic radii have been taken: Mo^{6+} = 0.62 Å, W^{6+} = 0.62 Å, Cl^- = 1.81 Å, and F^- = 1.33 Å. *Handbook of Chemistry and Physics*, 65th ed.; CRC Press: Boca Raton, FL, 1984.

(49) Nagarajan, G.; Adams, T. S. *Z. Phys. Chem.* **1974**, *255*, 869.

(50) McDowell, R. S.; Kennedy, R. C.; Asprey, L. B.; Sherman, R. J. *J. Mol. Struct.* **1977**, *36*, 1.

(51) Seip, H. M.; Seip, R. *Acta Chem. Scand.* **1966**, *20*, 2698.

(52) Figure 4 shows the eclipsed conformations (ν = 0) which exhibit the Laplacian distribution of the fluoride atoms.

corresponding molybdenum complexes **4a** and **4b** are not minima on the potential energy surface, which agrees with experimental observations.

Difluoroethyne is predicted to be more strongly bound in **5** and **6** than ethyne in **1a** and **2a**. The vinylidene isomers **7** and **9** are slightly higher in energy than the ethyne structures **1a** and **2a**, the energy difference being smaller for the molybdenum complex **9** than for the tungsten complex **7**. The fluorine-substituted vinylidene complexes **8** and **10**, however, are clearly lower in energy than the alkyne isomers **5** and **6**. The NBO analysis shows metal AO populations and partial charges which differ strongly from the formal d(0) population and the oxidation state +VI. Ethyne and vinylidene are calculated as being stronger acceptors (weaker donors) than chlorine. A comparison of the metal population in ML_6 and the corresponding ethyne complexes suggests that the complexes **1–10** should formally be considered as d(0) complexes with the oxidation state +VI. The valence AO configuration of the metal atoms is very similar in the hexahalides and in the complexes **1–10** derived from them. Two M–C bonds are predicted for the ethyne complexes, which indicates that **1–6** have cyclic structures and, therefore, should be considered as metallacyclopropenes. The M–C bonds in **1–6** are polarized toward the carbon end, the polarization being stronger in the tungsten complexes than in the molybdenum complexes. Two M–C bonds were also analyzed for the vinylidene complexes, one σ and one π bond. The former is clearly polarized toward the carbon end, but the polarization of the latter depends strongly on the metal and the ligands. The metal part of the M–C bond in **1–10** has mainly $(n-1)$d character. The topological analysis of the electronic structures shows a three-membered ring for the acetylene complexes and a partly covalent character of the M–C bonds, which is weak for the molybdenum alkyne complexes.

Acknowledgment. Stimulating discussions with Prof. K. Dehnicke are gratefully acknowledged. This work has been supported financially by the Fonds der Chemischen Industrie and the Deutsche Forschungsgemeinschaft (SFB 260). We acknowledge the helpful support by the computer centers of the Philipps Universität Marburg and the Hessischer Höchstleistungsrechner (HHLR), providing computer time on the Siemens S 400/40. Additional support was given by the computer companies Silicon Graphics and Convex.